



Adsorption of hydrogen on the surface and sub-surface of Cu(111)

Kumudu Mudiyanse, Yixiong Yang, Friedrich M. Hoffmann, Octavio J. Furlong, Jan Hrbek, Michael G. White, Ping Liu, and Darío J. Stacchiola

Citation: *The Journal of Chemical Physics* **139**, 044712 (2013); doi: 10.1063/1.4816515

View online: <http://dx.doi.org/10.1063/1.4816515>

View Table of Contents: <http://scitation.aip.org/content/aip/journal/jcp/139/4?ver=pdfcov>

Published by the [AIP Publishing](#)

Articles you may be interested in

[1,2-Dibromoethane on Cu\(100\): Bonding structure and transformation to C₂H₄](#)
J. Chem. Phys. **135**, 064706 (2011); 10.1063/1.3624348

[Adsorption of intact methanol on Ru\(0001\)](#)
J. Chem. Phys. **130**, 224703 (2009); 10.1063/1.3151674

[Vibrational properties of hydrogen atom adsorbed on Cu\(111\) and on Ir\(111\) surfaces](#)
J. Appl. Phys. **96**, 5020 (2004); 10.1063/1.1794905

[Adsorption of -pyridone on Cu\(110\)](#)
J. Chem. Phys. **116**, 8988 (2002); 10.1063/1.1471244

[Interaction of H atoms with Cu\(111\) surfaces: Adsorption, absorption, and abstraction](#)
J. Chem. Phys. **111**, 8115 (1999); 10.1063/1.480145



Re-register for Table of Content Alerts

Create a profile.



Sign up today!



Adsorption of hydrogen on the surface and sub-surface of Cu(111)

Kumudu Mudiyansele,¹ Yixiong Yang,² Friedrich M. Hoffmann,³ Octavio J. Furlong,⁴ Jan Hrbek,¹ Michael G. White,^{1,2} Ping Liu,¹ and Darío J. Stacchiola^{1,a)}

¹Chemistry Department, Brookhaven National Laboratory, Upton, New York 11973, USA

²Department of Chemistry, SUNY, Stony Brook, New York 11794, USA

³Department of Science, BMCC-CUNY, New York, New York 10007, USA

⁴INFAP/CONICET, Universidad Nacional de San Luis, Ejército de los Andes 950, 5700 San Luis, Argentina

(Received 26 March 2013; accepted 10 July 2013; published online 30 July 2013)

The interaction of atomic hydrogen with the Cu(111) surface was studied by a combined experimental-theoretical approach, using infrared reflection absorption spectroscopy, temperature programmed desorption, and density functional theory (DFT). Adsorption of atomic hydrogen at 160 K is characterized by an anti-absorption mode at 754 cm^{-1} and a broadband absorption in the IRRA spectra, related to adsorption of hydrogen on three-fold hollow surface sites and sub-surface sites, and the appearance of a sharp vibrational band at 1151 cm^{-1} at high coverage, which is also associated with hydrogen adsorption on the surface. Annealing the hydrogen covered surface up to 200 K results in the disappearance of this vibrational band. Thermal desorption is characterized by a single feature at $\sim 295\text{ K}$, with the leading edge at $\sim 250\text{ K}$. The disappearance of the sharp Cu-H vibrational band suggests that with increasing temperature the surface hydrogen migrates to sub-surface sites prior to desorption from the surface. The presence of sub-surface hydrogen after annealing to 200 K is further demonstrated by using CO as a surface probe. Changes in the Cu-H vibration intensity are observed when cooling the adsorbed hydrogen at 180 K to 110 K, implying the migration of hydrogen. DFT calculations show that the most stable position for hydrogen adsorption on Cu(111) is on hollow surface sites, but that hydrogen can be trapped in the second sub-surface layer. © 2013 AIP Publishing LLC. [<http://dx.doi.org/10.1063/1.4816515>]

I. INTRODUCTION

The interaction of hydrogen with metals is of great importance to many catalytic reactions including hydrogenation and dehydrogenation reactions, fuel cells, and hydrogen storage.^{1–3} Copper-based catalysts attract considerable interest due to their use in methanol synthesis,⁴ purification of hydrogen⁵ and unique reactivity for CO₂ electroreduction into hydrocarbon fuels.⁶ To obtain mechanistic insights of these reactions, fundamental understanding of the interactions of hydrogen with catalysts is essential. Even though hydrogen is the simplest atom, its interaction with transition metal surfaces is quite complex. The interaction of hydrogen with single crystal transition metals has been widely investigated (Ref. 7 and references therein), including Cu(111).^{7–30} The interaction of hydrogen with surfaces involves both adsorption onto the surface and absorption into the sub-surface. The study of sub-surface hydrogen is an active field, and it is been carried on a number of transition metals.^{7, 12, 14, 19, 25, 26, 31–37} For copper, and in particular on Cu(111), the role of sub-surface hydrogen is still not well understood.^{12, 14} Even though an early photoemission study by Plummer and Greuter¹¹ tentatively suggested that the binding energy of sub-surface sites is more favorable than that of surface sites, their subsequent electron energy loss spectroscopy study⁹ did not show evidence for the presence of

sub-surface hydrogen. Temperature programmed desorption (TPD) data have also been reported previously for the desorption of H from H/Cu(111).^{11, 13, 17, 19, 20} Lloyd *et al.* observed two desorption features, one at $\sim 200\text{ K}$ (α) and one at 300 K (β).¹⁹ The β -peak was assigned to surface hydrogen, whereas the α feature was associated to sub-surface hydrogen. In contrast, Luo *et al.* assigned the β feature to sub-surface hydrogen and the α to bulk hydrogen, based on the results from helium atom scattering (HAS) experiments.¹² Since helium atoms scatter off surfaces only, this method is extremely surface sensitive. They concluded that sub-surface absorption of hydrogen on Cu(111) is energetically favored in the limit of zero coverage and without surface reconstruction. These data are in conflict with earlier conclusions from TPD data, where the most stable adsorption site (β -300 K desorption) has been assigned to H adsorbed on the surface.^{17, 19, 20} Density functional theory (DFT) calculations predicted that sub-surface hydrogen is less stable than surface hydrogen.^{7, 22–24, 26}

Only a few studies have reported vibrational information for H/Cu(111) surfaces, with controversial results over the spectra and their assignments.^{9, 10, 18} The low dynamic dipole moment associated with the main metal-H stretch vibration, easily detected by high resolution electron energy loss spectroscopy (HREELS), has prevented its detection by infrared reflection absorption spectroscopy (IRRAS). Chabal *et al.* detected the presence of hydrogen on Mo(100) and W(100) by IRRAS, and assigned the observed sharp features to the overtone of the wagging mode from hydrogen adsorbed on bridge

^{a)} Author to whom correspondence should be addressed. Electronic mail: djs@bnl.gov

sites, coupled with sharp electronic surface states on molybdenum and tungsten.^{38–40}

In the present work we employed temperature programmed IRRAS (TP-IRRAS) in combination with TPD and DFT calculations to characterize the adsorption of hydrogen on Cu(111). Our data clearly show that surface hydrogen easily migrates to sub-surface sites prior to desorption from the β -state, and that hydrogen can be detected by IRRAS both in the sub-surface and surface.

II. EXPERIMENTAL AND THEORETICAL METHODS

Experiments were performed in a three level ultra-high vacuum (UHV) chamber (base pressure 2×10^{-10} Torr), which contains facilities for IRRAS, low energy electron diffraction (LEED), Auger electron spectroscopy (AES), and TPD. Vibrational spectra were obtained with a Bruker IFS/66v FTIR spectrometer at a resolution of 4 cm^{-1} .⁴¹ Time-evolved spectra were obtained by co-adding 100 scans at time intervals of 40 s, either at a constant temperature during exposure to hydrogen or in a temperature-programmed mode during slow heating of the sample with a linear heating rate of 0.1 K/s. TPD data were collected in a line-of-sight geometry with a UTI-100C mass spectrometer using a heating rate of 3 K/s. The sample mount allowed cooling to 90 K and heating to 1000 K using a programmable temperature controller. The Cu(111) sample was cleaned with argon ion sputtering followed by annealing to 800 K for 15 min. With the Cu(111) sample in the IRRAS position, the surface was exposed to atomic hydrogen at normal incidence from an atomic hydrogen source (Omicron “EFM H”) mounted in line-of-sight. Molecular hydrogen was introduced with a leak valve at the flange end of the atomic hydrogen source and pumped through the UHV chamber. During atomic hydrogen exposure the molecular hydrogen pressure was typically kept at 1×10^{-7} Torr (as measured in the UHV chamber), and exposures are quoted in Langmuirs of molecular hydrogen. The total hydrogen coverage was calculated correlating the molecular hydrogen exposure with the integrated intensity from subsequent TPDs, and referenced to the saturation coverage. The saturation coverage used in the current experiments corresponds to the full development of a (3×3) LEED pattern, which has been reported in the literature to be correlated with a hydrogen coverage of 0.67 ML.¹⁷

Unrestricted periodic DFT calculations were carried out using the code Dmol.^{42,43} The generalized gradient approximation (GGA) proposed by Perdew and Wang⁴⁴ was used for the exchange and correlation functional. The electron-ion interaction was described using effective core potentials. Wave functions were expanded in terms of a double-numerical basis set with a polarization d-function on all non-hydrogen atoms. A global orbital cutoff of 5.5 Å was employed. The Cu(111) surface was modeled by a five-layer slab with a (2×2) unit cell, separated by a 15 Å-thick vacuum layer. The bottom two layers of atoms were fixed in their optimized bulk positions. The top three layers were allowed to relax together with the adsorbates. Brillouin-zone integrations were conducted on a grid of $3 \times 3 \times 1$ Monkhorst-Pack special \mathbf{k} -points.⁴⁵

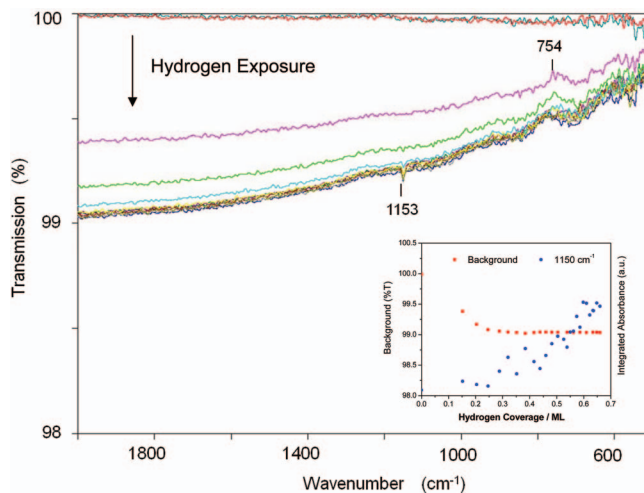


FIG. 1. Time-evolved transmission spectra illustrating the change in IR background during exposure of atomic hydrogen to Cu(111) at 180 K. Inset: plot of background transmission at 2000 cm^{-1} (red squares) and integrated absorbance of the 1150 cm^{-1} -band (blue circles) vs. total hydrogen coverage on Cu(111) at 180 K.

III. EXPERIMENTAL RESULTS

A. Broadband absorption and anti-absorption at low hydrogen exposures

Exposure of Cu(111) to atomic hydrogen results in a broadband absorption of the IR light, leading to a broad-band change of the IR background. Figure 1 shows IRRAS data obtained during exposure of Cu(111) to atomic hydrogen at 180 K. The data are displayed in transmittance mode (without background correction). The spectra show a broadband absorption, which increases for higher frequency (wavenumber). Broadband absorption has been observed previously for CO and NO on copper surfaces.⁴⁶ The theory proposed for this broadband absorption has been based on the surface resistivity concept,^{47,48} where the scattering of the metal conduction electrons from the adsorbate causes a broadband absorption of the IR light. Such broadband IR absorption has also been previously observed for saturation coverages of H and D adsorbed on Cu(111) in a (3×3) -layer by Lamont *et al.*¹⁰ Our data in Figure 1 show a similar broadband absorption as a function of increasing hydrogen exposure. The major change in the background occurs at total hydrogen coverage of ~ 0.3 ML, where the appearance of a (2×2) LEED pattern has been reported, and before the onset of a sharp band at $\sim 1150 \text{ cm}^{-1}$, which is discussed in detail in Sec. III B. The inset in Figure 1 shows a plot of the IR background change at 2000 cm^{-1} and the integrated absorbance of the 1150 cm^{-1} band as a function of total hydrogen coverage for the adsorption sequence in Figure 1. The data in Figure 1 also show an anti-absorption mode at 754 cm^{-1} , which seems to grow with the broadband absorption, but does not grow further as the 1150 cm^{-1} mode increases in intensity. An anti-absorption band at 770 cm^{-1} (590 cm^{-1} for D) was previously assigned to the parallel asymmetric stretch of H adsorbed on three-fold hollow sites by Lamont *et al.*¹⁰ Our data clearly indicate that the change in IR broadband absorption occurs largely at low exposure, where previous HREELS data have detected only

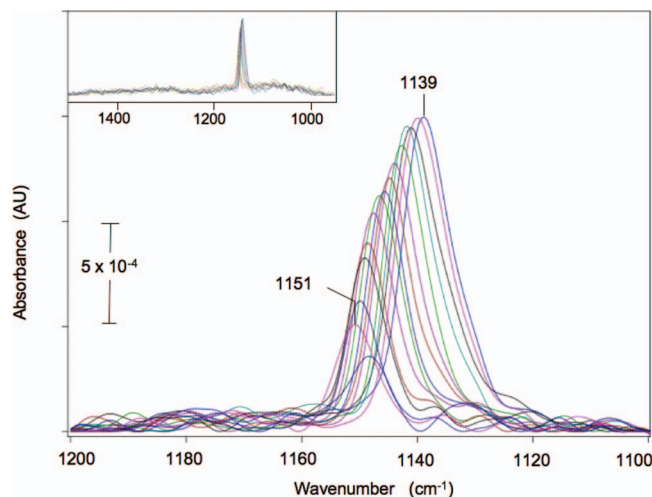


FIG. 2. Time-evolved IR spectra obtained during the adsorption of atomic hydrogen on Cu(111) at 160 K. Spectra were collected at 40 s time intervals, and the initial period without the peak at 1150 cm^{-1} has not been included. (Absorbance spectra are baseline corrected.) Inset: extended spectral range from 1500 to 950 cm^{-1} .

the presence of three-fold hollow site adsorbed hydrogen,⁹ but is not directly related to the growth of the IR band at 1150 cm^{-1} . We suggest that *the major change in broadband absorption at low exposure is related to a combination of adsorption of hydrogen on three-fold hollow sites on the surface and absorption in the sub-surface region.*

B. Adsorption of H at high exposures

Figure 2 presents time-evolved IR spectra obtained at 40 s time intervals during exposure of atomic hydrogen to Cu(111) at 160 K (termed “160 K-surface”). The first spectrum corresponds to the time where the peak at 1150 cm^{-1} is initially observed. The spectra are dominated by a single vibrational band (termed the “ 1150 cm^{-1} band”), which shifts with increasing exposure from 1151 to 1139 cm^{-1} and increases in half width (FWHM) from 7.5 to 10 cm^{-1} . The frequency is the same as the main feature observed by McCash *et al.* by IRRAS,¹⁸ with an even higher apparent intensity. The inset of Figure 2 displays the spectra from 950 to 1500 cm^{-1} , which show the absence of other significant absorption bands in this spectral range. In our study, this 1150 cm^{-1} peak appears after high exposures to atomic hydrogen at 160 K, following the initial occupation of hydrogen atoms on sub-surface and three-fold hollow surface sites. In order to further confirm that the peak at 1150 cm^{-1} is related to adsorbed H, we have performed experiments using deuterium. When pure deuterium was used, a sharp and intense feature at 870 cm^{-1} (see inset in Figure 4) was observed, which correlates with the isotope shift expected from the $\sim 1150\text{ cm}^{-1}$ peak from hydrogen adsorption. Based on the observed isotopic ratio of 1.32 this mode can be assigned to a vibration of hydrogen, as discussed further below.

Adsorption of hydrogen at 180 K results in similar vibrational spectra compared to those observed at 160 K in Figure 2. However, the intensity of the band observed at saturation is strongly reduced. A comparison of the integrated

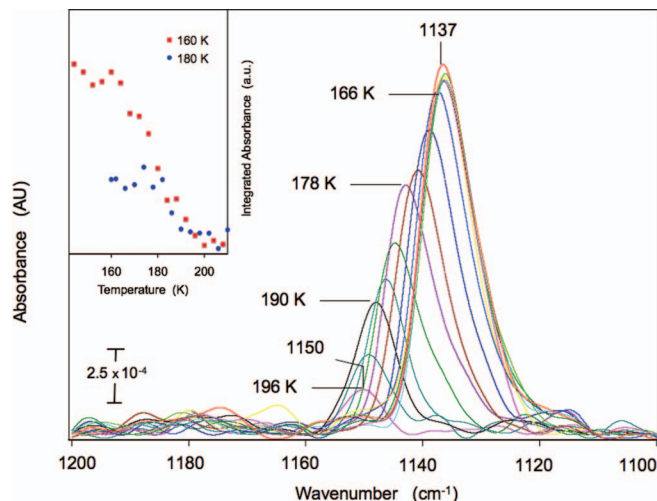


FIG. 3. Time-evolved IR spectra obtained for the 160 K-surface in Figure 2 during heating from 140 K to 200 K . (Heating rate = 0.1 K/s ; 4 K/spectrum .) Inset: integrated IR absorbance as a function of temperature for the 160 K-surface (red squares) and the 180 K-surface (blue circles). (Integration range from 1120 to 1160 cm^{-1} .)

intensity observed for adsorption at 160 K and 180 K shows that adsorption at 180 K results in saturation of the band intensity at approximately half of that of the 160 K surface.

C. Temperature-programmed IRRAS

Time-evolved IRRAS spectra obtained during heating of the H-saturated surface from 160 K to 220 K are presented in Figure 3. The vibrational spectra show that heating above 170 K results in the decrease of IR intensity and the eventual disappearance of the IR band at 200 K. Simultaneously with the decrease in IR intensity, the band’s frequency shifts from 1137 to 1150 cm^{-1} , reversing the shift observed during adsorption. The plot of the integrated absorbance as a function of temperature, in the inset of Figure 3 (red squares), shows the onset of the intensity decrease at 165 K, and the virtual disappearance of the band at 200 K. A comparison with the heating sequence of the 180 K-surface (blue circles) shows almost identical behavior with a temperature range of 185 – 200 K for the disappearance of the 1150 cm^{-1} band. We note that both for the 160 K- and the 180 K-surface, heating does not result in a significant change in linewidth ($<1\text{ cm}^{-1}$). This is important, since it implies that the disappearance of the IR band is not related to vibrational dephasing at higher temperature, which could result in band broadening such that the band disappears below the noise level.

D. Thermal desorption

A TPD spectrum obtained from a Cu(111) surface saturated with atomic deuterium at 160 K is shown in Figure 4 (a similar spectrum was observed from a Cu(111) surface saturated with atomic H). The spectrum has a strong and broad peak at 296 K, denoted as β -state, and has been reported in previous studies.^{17,19,20} Anger *et al.*²⁰ found this peak to follow second-order desorption kinetics with a

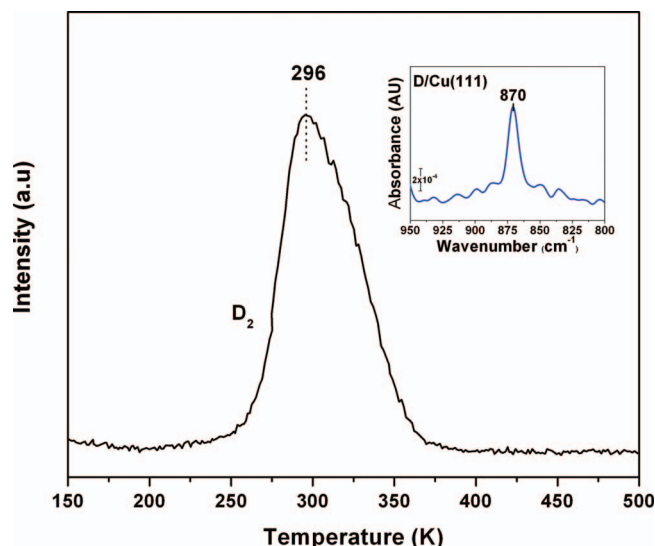


FIG. 4. Thermal desorption spectrum (mass 4) after the adsorption of a saturation coverage of deuterium on Cu(111) at 160 K. (Heating rate = 3 K/s). The corresponding IR spectrum is shown in the inset.

coverage-dependent desorption energy of 20 to 15 kcal/mol. The β -state was assigned to desorption of hydrogen from the surface.^{17,19,20} At higher exposures two additional desorption features, α_1 and α_2 , were observed at 200 and 220 K, respectively, by Lloyd *et al.*¹⁹ The α_1 -state saturated at about one half of the coverage of the β -state and was assigned to H adsorbed in sub-surface sites. The α_2 -state, which did not saturate, exhibited zero-order kinetics and was assigned to hydrogen adsorbed in the bulk. A different assignment for the β -state has been suggested by Luo *et al.*^{12,14} Based on HAS experiments discussed in detail below, these authors found that surface hydrogen is not stable at low coverage and higher temperature (>200 K), which lead them to conclude that the β -state is not due to desorption of surface hydrogen, but to first-order desorption from *sub-surface* hydrogen.

A comparison of the vibrational data from TP-IRRAS (Figure 3) with the TPD data (Figure 4) reveals an absence of causative link between the disappearance of the Cu-H vibration and the desorption of hydrogen from Cu(111). The vibrational data show that the band at 1150 cm^{-1} disappears at 200 K (Figure 3), whereas the major desorption peak in TPD occurs $\sim 100\text{ K}$ higher at 296 K (Figure 4), with its leading edge at $\sim 250\text{ K}$. Note that this 100 K difference cannot be due to the difference in heating rates between TP-IRRAS and TPD (0.1 K/s vs. 3 K/s), since the latter would result in a much smaller shift of 10–20 K to lower temperature.⁴⁹ A TPD experiment performed right after observing the disappearance of the $\sim 1150\text{ cm}^{-1}$ feature shows the same desorption peak of H_2 observed without the intermediate annealing step. This clearly demonstrates that *the disappearance of the 1150 cm^{-1} band in IRRAS is not related to desorption of hydrogen from the surface.* Since no other significant desorption peak is observed below 250 K in Figure 4, we conclude that the H is still present on the sample in a form which is not visible in IRRAS. Thermally activated hydrogen migration to form structures with no dipole moment perpendicular to the surface could make hydrogen invisible. The probable arrange-

ment is the formation of sub-surface hydrogen. A similar conclusion has been reported by Luo *et al.*^{12,14} Based on helium atom scattering, an experimental technique of exclusive surface sensitivity, and TPD data, these authors have shown that hydrogen disappears from the surface between 180 and 250 K, i.e., before the onset of the desorption from the β -state observed with TPD at 300 K. Based on their data, these authors found that *hydrogen adsorbed on the surface is thermodynamically not stable at 210–245 K*, and conclude that H atoms are transported from the surface to sub-surface sites by an activated process.

E. CO adsorption as a surface probe

Direct observation of a vibrational mode assigned to sub-surface hydrogen adsorbed on metal surfaces has been reported only in one case.⁵⁰ Utilizing HREELS in specular and off-specular geometries and thermal desorption, Johnson *et al.* observed the adsorption of atomic hydrogen on Ni(111) in two bonding states. A strongly adsorbed state, desorbing at 320–380 K, was characterized by an energy loss at 144 meV (1161 cm^{-1}) in dipole scattering, and was assigned to the Ni–H stretch mode of surface hydrogen. A second weaker state with a desorption temperature of $\sim 200\text{ K}$ and an energy loss at 99 meV (798 cm^{-1}) was only observed with impact scattering indicating a dipole-forbidden mode which was assigned to sub-surface hydrogen. Therefore, we use an indirect method for further confirmation of the presence of sub-surface H.

In order to interrogate the surface for the presence of H we used CO as a probe molecule, since the presence of H atoms can strongly affect the adsorption of CO by weakening the Cu–CO bond and suppressing CO adsorption. Figure 5 shows IRRAS spectra obtained for different states of the H-Cu(111) surface. Spectrum (a) was obtained after exposure of atomic hydrogen to Cu(111) at 160 K and subsequent exposure to CO at 105 K. We observe two bands due to a Cu–H vibration at 1132 cm^{-1} and a C–O stretching vibration at 2059 cm^{-1} . This spectrum is characteristic of the co-adsorbed CO and H, as it shows that the presence of surface H suppresses the adsorption of CO. The C–O band is shifted to lower frequency and its intensity is strongly reduced compared to that of a saturation coverage of CO on clean Cu(111). Heating of the surface to 200 K results in the complete desorption of CO and the disappearance of the Cu–H vibration band. Spectrum (b) was obtained after re-adsorption of CO and re-cooling to 95 K. The H band at 1132 cm^{-1} has virtually disappeared, but CO adsorption is still strongly suppressed as indicated by the reduced intensity of the C–O band at 2058 cm^{-1} . The latter band is also accompanied by several small bands at higher frequencies ($2095\text{--}2120\text{ cm}^{-1}$), similar to the previously reported results by King *et al.* on the formation of electronically modified atop adsorption sites for co-adsorbed CO and H on Ni(110).⁵¹ Since the diffraction HAS data do not show any evidence of surface reconstruction due to sub-surface hydrogen,^{12,14} it appears likely that these bands are due to the electronic modification of the surface by the presence of sub-surface hydrogen. The observed shift in frequency above 2100 cm^{-1} is consistent with CO adsorbed

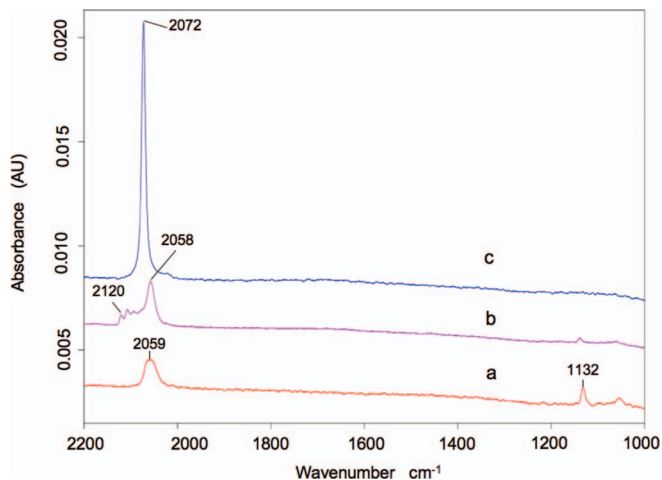


FIG. 5. (a) CO adsorption on a H-Cu(111) surface during cooling to 105 K (see text for details). (b) CO adsorption after TP-IRRAS to 220 K and during re-cooling to 95 K. (c) CO adsorption after heating to 310 K and re-cooling to 104 K. (a)-(c) $P_{\text{CO}} = 1 \times 10^{-8}$ Torr CO.

at electron deficient $\text{Cu}^{\delta+}$ sites of a hydride-like layer. Heating of the surface beyond desorption of the β -state to 310 K and exposure of the surface to CO at 105 K results in spectrum (c). We observe a substantial increase of the intensity of the C–O band and a shift to 2072 cm^{-1} , with both intensity and frequency being characteristic of CO adsorbed on clean Cu(111).^{52,53}

The data presented in Figure 5 corroborate the conclusion we reached after collecting and interpreting the TP-IRRAS and TPD data: there is clear evidence that the disappearance of surface hydrogen after heating to 220 K is not related to desorption of hydrogen. Therefore, the disappearance of the surface hydrogen must be attributed to the transfer of hydrogen to sub-surface sites. This mechanism has been suggested earlier by Luo *et al.*,^{12,14} who demonstrated with helium atom scattering data that at elevated temperatures ($>200 \text{ K}$) adsorbed hydrogen is transported from surface to sub-surface sites in an activated process, as discussed above. This model for the disappearance of surface hydrogen by transfer to the sub-surface is further corroborated by vibrational data, which can only be understood in the context of this model.

F. Diffusion of sub-surface hydrogen to the surface sites

Figure 6 presents vibrational data obtained after exposure of atomic hydrogen to Cu(111) at 180 K and subsequent cooling of the surface to 110 K. A strong increase in intensity of the Cu–H band at 1150 cm^{-1} is observed during this process. A plot of the integrated absorbance in the inset of Figure 6 shows an increase of $\sim 50\%$. We attribute this increase in band intensity to a transfer of sub-surface hydrogen back to the surface with decreasing surface temperature. We also note that the intensity increase is accompanied by a change in lineshape of the band, which is more asymmetric at 180 K than after cooling to 110 K. The asymmetry at the higher temperature results from a more inhomogeneous layer due to the presence of hydrogen in the sub-surface region. Al-

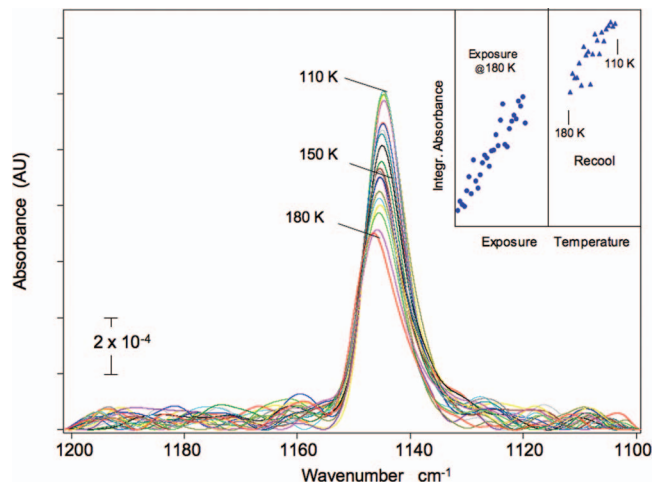


FIG. 6. IR spectra obtained after adsorption of H at 180 K and re-cooling of the surface from 180 K to 110 K. Inset: integrated absorbance as a function of exposure (left) and recooling (right).

ternatively, the band asymmetry could also be a result of the segregation of surface H into two regions of different coverage. However, the latter is less likely in our view, since such a segregation is more likely to occur upon *cooling* the surface, as observed, for example, for CO adsorbed on Ru(001).⁵⁴

IV. DFT CALCULATION RESULTS

In our calculations, the interaction of atomic hydrogen with Cu(111) was modeled at the saturation coverage (0.75 mono layers-ML), where the possible adsorption sites for the hydrogen atoms are on the surface (SH), in the sub-surface between the surface layer and the first sub-surface layer (SSH-1st), and in the sub-surface between the first and the second sub-surface layer (SSH-2nd). Note that in these calculations we do not consider hydrogen adsorbed on weaker surface adsorption sites, since their concentration would be lower than that of H on fcc and sub-surface sites, and its diffusion to sub-surface sites would proceed through the more stable three-fold hollow sites. The binding energy is defined as: $E_b = E[3\text{H}/\text{Cu}(111)] - E[\text{Cu}(111)] - 1.5 \times E[\text{H}_2(\text{g})]$. The results of our calculations, presented in Figure 7, show that the surface sites ($E_b = -0.85 \text{ eV}$) are more favorable than sub-surface sites for the adsorption of hydrogen, which is in agreement with previously reported calculations using low hydrogen coverages.^{7,22–24,26,29} There are two other adsorption configurations, which lead to an exothermic process. One corresponds to the case with 0.25 ML of SSH-1st and 0.50 ML of SH atoms; the other represents 0.25 ML of SSH-2nd and 0.50 ML of SH (Figure 7). The calculated adsorption energies for both cases are negative and very similar in magnitude ($\sim -0.35 \text{ eV}$). As shown in Figure 7, the diffusion barrier for SSH-2nd \rightarrow SSH-1st is 0.24 eV, while there is practically no barrier for SSH-1st \rightarrow SH (0.03 eV). That is, during the process of SH penetration to the sub-surface, SSH-1st is the least stable and therefore present at only small concentrations, while SSH-2nd may be trapped by the larger activation barrier and be observable experimentally. It seems possible for an incident atomic H to penetrate and populate the sub-surface

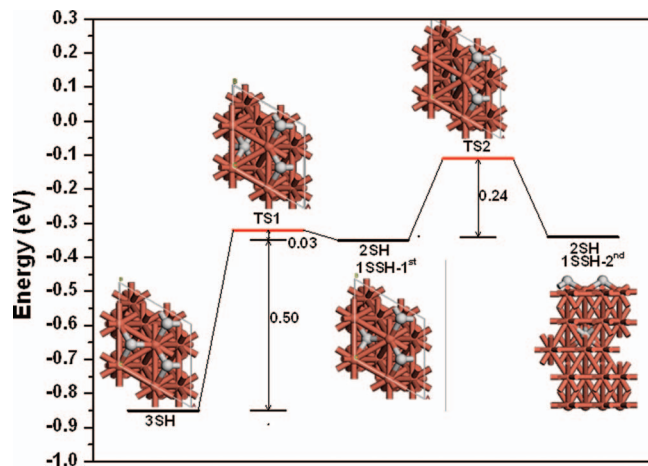


FIG. 7. Potential energy diagram for the adsorption and absorption of H at high coverage (3 hydrogen atoms per unit cell). The top view of the optimized structures for the 3SH, TS1, 2SH + 1SSH-1st, TS2 systems, and the side view of the 2SH + 1SSH-2nd system are also shown. SH-surface H, SSH-1st – H between the surface layer and the first sub-surface layer, SSH-2nd – H between the first and the second sub-surface layer (SSH-2nd), TS-transition state. Big brown: Cu; small white: H.

sites at elevated temperatures, though the overall reaction, SH \rightarrow SSH-2nd, is endothermic with an enthalpy change (ΔH) of 0.50 eV. Our experimental results are in agreement with this prediction and clearly show that atomic hydrogen adsorbed at 160–180 K has enough energy to penetrate through the surface and populate the sub-surface sites.

The transition from SH \rightarrow SSH-1st is the rate limiting step in the diffusion of hydrogen into the bulk, and the activation energy E_a for this process can be evaluated experimentally with an Arrhenius plot, using the coverage of SH measured in Figure 3:

$$\frac{d \ln k}{d(1/T)} = -\frac{E_a}{R}.$$

The total hydrogen coverage is maintained constant, since no desorption of hydrogen is observed in the 160–200 K temperature region with TPD experiments. The result is presented in Figure 8 ($E_a = 0.55 \pm 0.05$ eV), where a good agreement is obtained with our calculated value of 0.53 eV (Figure 7) and from HAS experiments using typical pre-exponential factors (0.66 eV).¹⁴

Based on the energy diagram shown in Figure 7, we can now explain the experimental results described above. Atomic hydrogen dosed to the Cu(111) surface is absorbed initially in the SSH-2nd sites, due to the kinetic energy of the impinging H atoms produced by the hot capillary source. As the hydrogen concentration increases, a temperature-dependent equilibrium is reached in the occupation of SH and SSH-2nd sites. The occupation of SSH-1st sites is always very small, due to the facile diffusion of sub-surface H atoms to SH sites. When the adsorption of H is carried out at higher temperatures the surface/sub-surface concentration equilibrium is shifted towards the SSH-2nd sites. Cooling the sample moves the equilibrium back towards the SH sites, as seen in Figure 6. During the annealing of H-covered surfaces, above 200 K the equilibrium shifts to primarily sub-surface occupancy in

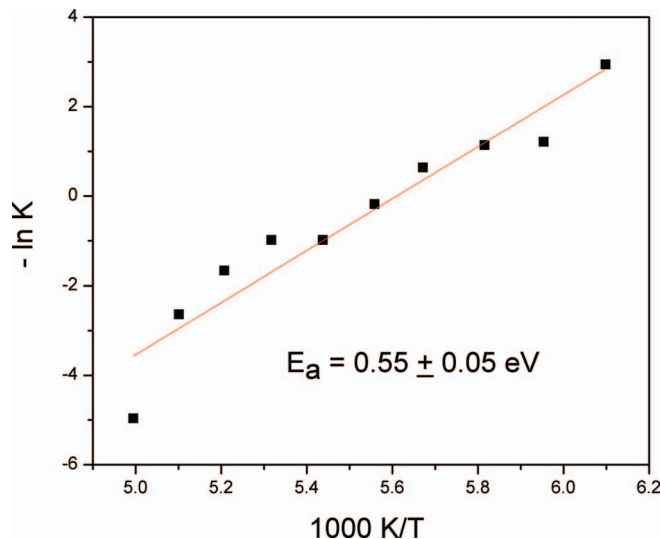


FIG. 8. Experimental E_a calculation between SH and SSH-1st sites, from the SH coverage measurements in the inset of Figure 3.

SSH-2nd or deeper into the bulk sites. Further annealing leads to H recombination to form H_2 in a reaction limited step with a desorption peak at ~ 290 K in the TPD spectrum. The entire process is possible due to the asymmetric nature of the activation barrier for diffusion between SH \leftrightarrow SSH-2nd.

V. DISCUSSION ABOUT VIBRATIONAL ASSIGNMENTS

There is only one vibrational study report on the Cu–H system, where hydrogen was observed by both IRRAS and HREELS.¹⁸ A tentative assignment of the peaks was proposed, relating the most intense and sharp peak in the IRRAS spectra at 1151 cm^{-1} to an overtone of the wagging mode from hydrogen adsorbed on bridging sites, based on the assignment by Chabal *et al.* described above, and the other observed at $\sim 1040 \text{ cm}^{-1}$ on both IRRAS (weak and broad) and HREELS (strong) to the stretching mode of Cu–H in a two-fold bridge site. However, the assignment corresponding to the stretching mode of bridge bonded hydrogen was contradicted by calculated vibrational frequencies for hydrogen on hollow and bridge sites of Cu(111).²¹ Later HREELS data for the same Cu–H(D) system have shown one major loss at $\sim 1040 \text{ cm}^{-1}$ (774 cm^{-1}), which was assigned to the Cu–H(D) vibration in three-fold hollow sites, in disagreement with the previous assignment, and one feature at $\sim 927 \text{ cm}^{-1}$ (661 cm^{-1}) for high coverage, which was tentatively assigned to sub-surface hydrogen.⁹ A synchrotron IR study found an anti-absorption feature at 770 cm^{-1} , which was assigned to the asymmetric stretch mode (parallel to the surface) of hydrogen adsorbed on three-fold hollow sites, but did not observe any bands above 800 cm^{-1} due to instrumental limitations, neither clear evidence of the stretch mode from deuterium below 800 cm^{-1} .¹⁰ The dipole forbidden vibration (the parallel asymmetric stretch hydrogen mode) could only be observed due to its coupling to electrons from the copper substrate.^{10,47}

The appearance of the sharp peak at 1150 cm^{-1} (870 cm^{-1}) for H(D) adsorption at high coverage on Cu(111)

is similar to the results reported by Chabal *et al.* for H on Mo(100) and W(100),^{38–40} assigned to an overtone of the wagging mode from hydrogen adsorbed on a bridge site. The enhanced intensity of those overtone peaks was attributed to their coupling with sharp surface-electronic states, and could only be observed by IRRAS but not by HREELS.⁴⁰ HREELS is in turn very sensitive to the corresponding stretching modes. Plummer and Lee observed a peak at 115 meV (82 meV) [927 cm⁻¹ (661 cm⁻¹)] for the H(D)/Cu(111) system at high coverages, after the (3 × 3) LEED pattern appeared, which was tentatively assigned to sub-surface hydrogen.⁹ This feature matches the 117 meV (85 meV) main vibrational feature assigned to the symmetric stretching mode of bridging hydrogen on the reconstructed Cu(100) surface by HREELS.⁵⁵ Therefore, the 1150 cm⁻¹ peak observed at high coverage of hydrogen on Cu(111) could be related to adsorption on weaker two-fold bridge sites. Alternatively, the 1150 cm⁻¹ (870 cm⁻¹) peak could be related to the vibrational coupling between surface and sub-surface H (D) atoms. In any case, there is no doubt of its relation to the presence of surface hydrogen, indicating the possibility of the direct detection of this elusive species by IRRAS.

VI. CONCLUSIONS

In summary, vibrational and thermal desorption data provide clear evidence that atomic hydrogen adsorbed on Cu(111) can occupy both surface and sub-surface sites:

- (i) Based on vibrational TP-IRRAS data we observe the disappearance of *surface* hydrogen at much lower temperature than its desorption from the β -state, which is observed in TPD at 296 K.
- (ii) The adsorption of CO, used as a surface probe, is suppressed by the presence of both surface and sub-surface hydrogen.
- (iii) Adsorption of hydrogen at 180 K results in a strongly reduced intensity of the Cu–H vibration at 1150 cm⁻¹, but after re-cooling to 110 K the band intensity increases commensurate with a *transfer of sub-surface hydrogen back to the surface*.
- (iv) A broadband absorption observed at low exposure, *before the onset of the 1150 cm⁻¹ band*, suggests the absorption of hydrogen in the sub-surface region even at low coverages.
- (v) DFT calculations demonstrate the presence of sub-surface hydrogen between the first and the second sub-surface layer (SSH-2nd), rationalizing our current experimental results and some inconsistencies previously reported in the literature.

ACKNOWLEDGMENTS

The work carried out at the Brookhaven National Laboratory was supported by the US Department of Energy (DOE) (Chemical Sciences Division, DE-AC02-98CH10886). The DFT calculations were carried out using the computing facility at the Center for Functional Nanomaterials at Brookhaven National Laboratory.

- ¹I. Chorkendorff and H. Niemantsverdriet, *Concepts of Modern Catalysis and Kinetics* (Wiley-VCH, Weinheim, Germany, 2003).
- ²C. N. Satterfield, *Heterogeneous Catalysis in Industrial Practice*, 2nd ed. (Krieger Publishing Company, Malabar, FL, 1996).
- ³*Hydrogen in Metals II: Application-Oriented Properties*, edited by G. Alefeld and J. Völkl (Springer-Verlag, Berlin, 1978).
- ⁴M. Behrens, F. Studt, I. Kasatkin, S. Kuhl, M. Havecker, F. Abild-Pedersen, S. Zander, F. Girgsdies, P. Kurr, B. L. Knief, M. Tovar, R. W. Fischer, J. K. Nørskov, and R. Schlögl, *Science* **336**, 893–897 (2012).
- ⁵K. Mudiyansele, S. D. Senanayake, L. Feria, S. Kundu, A. E. Baber, J. Graciani, A. B. Vidal, S. Agnoli, J. Evans, R. Chang, S. Axnanda, Z. Liu, J. F. Sanz, P. Liu, J. A. Rodriguez, and D. J. Stacchiola, *Angew. Chem., Int. Ed.* **52**, 5101–5105 (2013).
- ⁶A. A. Peterson, F. Abild-Pedersen, F. Studt, J. Rossmeisl, and J. K. Nørskov, *Energy Environ. Sci.* **3**, 1311–1315 (2010).
- ⁷P. Ferrin, S. Kandoi, A. U. Nilekar, and M. Mavrikakis, *Surf. Sci.* **606**, 679–689 (2012).
- ⁸A. D. Jewell, G. W. Peng, M. F. G. Motta, E. A. Lewis, C. J. Murphy, G. Kyriakou, M. Mavrikakis, and E. C. H. Sykes, *ACS Nano* **6**, 10115–10121 (2012).
- ⁹G. Lee and E. W. Plummer, *Surf. Sci.* **498**, 229–236 (2002).
- ¹⁰C. L. A. Lamont, B. N. J. Persson, and G. P. Williams, *Chem. Phys. Lett.* **243**, 429–434 (1995).
- ¹¹F. Greuter and E. W. Plummer, *Solid State Commun.* **48**, 37–41 (1983).
- ¹²M. F. Luo, D. A. MacLaren, I. G. Shuttleworth, and W. Allison, *Chem. Phys. Lett.* **381**, 654–659 (2003).
- ¹³T. Kammler and J. Kupperts, *J. Chem. Phys.* **111**, 8115–8123 (1999).
- ¹⁴M. F. Luo, D. A. MacLaren, and W. Allison, *Surf. Sci.* **586**, 109–114 (2005).
- ¹⁵S. Caratzoulas, B. Jackson, and M. Persson, *J. Chem. Phys.* **107**, 6420–6431 (1997).
- ¹⁶C. T. Rettner, *Phys. Rev. Lett.* **69**, 383–386 (1992).
- ¹⁷G. Lee, D. B. Paker, D. M. Zehner, and E. W. Plummer, *Surf. Sci.* **357–358**, 717–720 (1996).
- ¹⁸E. M. McCash, S. F. Parker, J. Pritchard, and M. A. Chesters, *Surf. Sci.* **215**, 363–377 (1989).
- ¹⁹P. B. Lloyd, M. Swaminathan, J. W. Kress, and B. J. Tatarchuk, *Appl. Surf. Sci.* **119**, 267–274 (1997).
- ²⁰G. Anger, A. Winkler, and K. D. Rendulic, *Surf. Sci.* **220**, 1–17 (1989).
- ²¹K. Gundersen, B. Hammer, K. W. Jacobsen, J. K. Nørskov, J. S. Lin, and V. Milman, *Surf. Sci.* **285**, 27–30 (1993).
- ²²J. Strömquist, L. Bengtsson, M. Persson, and B. Hammer, *Surf. Sci.* **397**, 382–394 (1998).
- ²³K. Nobuhara, H. Nakanishi, H. Kasai, and A. Okiji, *Surf. Sci.* **493**, 271–277 (2001).
- ²⁴J. Greeley and M. Mavrikakis, *J. Phys. Chem. B* **109**, 3460–3471 (2005).
- ²⁵M. F. Luo, G. R. Hu, and M. H. Lee, *Surf. Sci.* **601**, 1461–1466 (2007).
- ²⁶M. F. Luo and G. R. Hu, *Surf. Sci.* **603**, 1081–1086 (2009).
- ²⁷K. Nobuhara, H. Nakanishi, H. Kasai, and A. Okiji, *J. Appl. Phys.* **88**, 6897–6901 (2000).
- ²⁸K. Nobuhara, H. Kasai, H. Nakanishi, and W. A. Dino, *J. Appl. Phys.* **96**, 5020–5025 (2004).
- ²⁹J. L. Nie, H. Y. Xiao, and X. T. Zu, *Chem. Phys.* **321**, 48–54 (2006).
- ³⁰K. Christmann, *Surf. Sci. Rep.* **9**, 1–163 (1988).
- ³¹W. Eberhardt, F. Greuter, and E. W. Plummer, *Phys. Rev. Lett.* **46**, 1085–1088 (1981).
- ³²G. E. Gdowski, T. E. Felter, and R. H. Stulen, *Surf. Sci. Lett.* **181**, L147–L155 (1987).
- ³³D. E. Jiang and E. A. Carter, *Surf. Sci.* **547**, 85–98 (2003).
- ³⁴J. T. Yates, Jr., C. H. F. Peden, J. E. Houston, and D. W. Goodman, *Surf. Sci.* **160**, 37–45 (1985).
- ³⁵R. Löber and D. Hennig, *Phys. Rev. B* **55**, 4761–4765 (1997).
- ³⁶D. Stacchiola and W. T. Tysoe, *Surf. Sci.* **540**, L600–L604 (2003).
- ³⁷R. J. Behm, V. Penka, M. G. Cattania, K. Christmann, and G. Ertl, *J. Chem. Phys.* **78**, 7486–7490 (1983).
- ³⁸Y. J. Chabal, *Phys. Rev. Lett.* **55**, 845–848 (1985).
- ³⁹J. E. Reutt, Y. J. Chabal, and S. B. Christman, *J. Electron. Spectrosc. Relat. Phenom.* **44**, 325–332 (1987).
- ⁴⁰J. E. Reutt, Y. J. Chabal, and S. B. Christman, *Phys. Rev. B* **38**, 3112–3132 (1988).
- ⁴¹J. Hrbek, F. M. Hoffmann, J. B. Park, P. Liu, D. Stacchiola, Y. S. Hoo, S. Ma, A. Nambu, J. A. Rodriguez, and M. G. White, *J. Am. Chem. Soc.* **130**, 17272–17273 (2008).
- ⁴²B. Delley, *J. Chem. Phys.* **92**, 508–517 (1990).

- ⁴³B. Delley, *J. Chem. Phys.* **113**, 7756–7764 (2000).
- ⁴⁴J. P. Perdew, J. A. Chevary, S. H. Vosko, K. A. Jackson, M. R. Pederson, D. J. Singh, and C. Fiolhais, *Phys. Rev. B* **46**, 6671 (1992).
- ⁴⁵H. J. Monkhorst and J. D. Pack, *Phys. Rev. B* **13**, 5188 (1976).
- ⁴⁶C. J. Hirschmugl, G. P. Williams, F. M. Hoffmann, and Y. J. Chabal, *Phys. Rev. Lett.* **65**, 480–483 (1990).
- ⁴⁷B. N. J. Persson, *Phys. Rev. B* **44**, 3277–3296 (1991).
- ⁴⁸B. N. J. Persson and A. I. Volokitin, *Surf. Sci.* **310**, 314–336 (1994).
- ⁴⁹P. A. Redhead, *Vacuum* **12**, 203–211 (1962).
- ⁵⁰A. D. Johnson, K. J. Maynard, S. P. Daley, Q. Y. Yang, and S. T. Ceyer, *Phys. Rev. Lett.* **67**, 927–930 (1991).
- ⁵¹J. G. Love, S. Haq, and D. A. King, *J. Chem. Phys.* **97**, 8789–8797 (1992).
- ⁵²P. Hollins and J. Pritchard, *Surf. Sci.* **89**, 486–495 (1979).
- ⁵³K. Mudiyanselage, W. An, F. Yang, P. Liu, and D. J. Stacchiola, *Phys. Chem. Chem. Phys.* **15**, 10726–10731 (2013).
- ⁵⁴H. Pfnür, D. Menzel, F. M. Hoffmann, A. Ortega, and A. M. Bradshaw, *Surf. Sci.* **93**, 431–452 (1980).
- ⁵⁵I. Chorkendorff and P. B. Rasmussen, *Surf. Sci.* **248**, 35–44 (1991).